IEEE Access
Multidisciplinary ⋮ Rapid Review ⋮ Open Access Journal

Received April 27, 2021, accepted May 6, 2021, date of publication May 17, 2021, date of current version May 26, 2021.

Digital Object Identifier 10.1109/ACCESS.2021.3081152

Real-Time Direction Judgment System of Sub-Nanometer Scale Grating Ruler

SIMIN LI[1], JINGKUN WANG[2], WENTAO ZHANG[2], HAO DU[2], AND XIANMING XIONG[2]
[1]College of Electrical and Information Engineering, Guangxi University of Science and Technology, Liuzhou 545000, China
[2]College of Electronic Engineering and Automation, Guilin University of Electronic Technology, Guilin 541000, China

Corresponding author: Wentao Zhang (glietzwt@163.com)

This work was supported in part by the National Science and Technology Major Project under Grant 2017ZX02101007-003, in part by the National Natural Science Foundation of China under Grant 61965005, in part by the Natural Science Foundation of Guangxi Province under Grant 2019GXNSFDA185010, and in part by the Guilin University of Electronic Technology Postgraduate Training Program under Grant 18YJPYBS02. The work of Wentao Zhang was supported in part by the Guangxi Distinguished Expert Project.

ABSTRACT This paper presents the design of a real-time direction judgment system for a sub-nanometer scale grating ruler based on field-programmable gate array (FPGA) technology. On the basis of the working principle of the grating ruler reading head, the characteristics of the grating ruler phase signal are analyzed. In view of the frequency uncertainty and nonlinear error of grating scale phase signal laser, a preprocessing structure based on biorthogonal lock-in amplifier is designed. Aiming at the problem of low data update rate and insensitivity to direction switching in short stroke of traditional grating direction judgment method, a real-time direction judgment method is proposed. On the FPGA platform, the signal generator is used to simulate the actual photoelectric signal of grating ruler, and the calibration experimental platform of electrical analog signal is built to verify the effect of the real-time direction judgment system on the FPGA platform. The results show that compared with the traditional direction judgment system, the data update rate is improved by 256-fold. Moreover, a method for using the result of the direction judgment system to compensate the count value of the electronic subdivision when the object is moving backward is proposed.

INDEX TERMS Direction judgment, grating ruler, electronic subdivision, FPGA implementation.

I. INTRODUCTION

With the increasing development of science and technology, the requirement for precise measurements in the field of industrial production has increased. Facing these requirements, many high-precision measurement technologies have appeared, one of which is the sub-nanometer scale grating ruler [1]–[2].

The two most common high-precision sensors are the interferometer and grating ruler [3]–[6]. The grating ruler has a short optical path that makes it robust to the environment. Thus, a grating ruler can provide a higher measurement stability [7]–[9]. As a high-precision measurement sensor, a sub-nanometer scale grating ruler is widely used in various areas such as radar, computer numerical control, and semiconductor processing [10]–[13].

At present, methods for identifying the direction of a grating ruler signal can be roughly divided into three categories. The first is to lay out the photoelectric detector at equal space of the grating movement track and determine the grating movement direction according to the changing trend of the detection signal of the photoelectric detector [14]. However, the resolution of this method depends on the number and density of the photodetectors installed. With improvements in the measurement accuracy, the data update rate of the direction judgment should also be improved, which implies that the cost and installation difficulties of the photodetectors will exponentially increase.

The second is the direction judgment method based on sine and cosine symbol bits, which reflects the raster motion through the changing trend of the sine and cosine input signal symbol bits [15]. When the grating is moving forward, the phase of the sine signal is in advance of the cosine signal phase by 90°. In a cycle, the symbol bits of the input signal have four relative changes: 00→10→11→01→00. It can be observed that the grating ruler moves forward when two adjacent signals appear in the four groups of signals. When the grating is moving backward, the phase of sine lags behind cosine phase by 90°. The symbol bits of the input signal also have four relative changes: 00→01→11→10→00. It can be

The associate editor coordinating the review of this manuscript and approving it for publication was Leonel Sousa.

observed that the grating ruler moves backward when two adjacent signals appear in the four groups of signals.

The third class is based on a phase-shift circuit [16]. By shifting the phase of the input signal, multi-channel signals with different phases are output. The direction judgment results are obtained according to the phase advance information of each channel.

When the optical subdivision method was used in the previously mentioned grating scale, and the subdivision multiple was 4, the above four methods showed an excellent direction judgment effect. However, with the development of the electronic subdivision, the digital subdivision method based on amplitude can perform 1024 subdivisions or higher. The result of the direction judgment cannot be replaced for compensating the quadrant judgment in CORDIC algorithm and the final phase results. Moreover, the traditional method updates the result of the direction judgment every 1/4 period, which cannot meet the real-time requirements of a grating ruler with a high fine fraction. Once the object moves back and forth within a range of a quarter grating pitch, misjudgments easily occur in traditional direction judgment systems, thereby affecting the accuracy of the measurement.

To meet the real-time requirement of a high-precision measurement for direction judgment, a research was conducted on real-time direction judgment systems based on FPGA technology, which can be applied to measurement boards, and can be helpful in providing a resolution of $\lambda/1024$ or even higher.

II. WORKING PRINCIPLE OF GRATING RULER

The measurement system used in this study applies a ZMI 7702 laser head to generate dual-frequency laser beams with a difference in frequency of 20 MHz.

The nominal vacuum wavelength was 633 nm. When the laser beams enter the grating surface, diffracted light of different orders is produced according to the diffraction characteristics of the grating [17], as shown in Figure 1.

The displacement of the plane grating is obtained by calculating the Doppler shift of the diffracted light. In order to improve the measurement resolution, the higher diffraction times should be selected as far as possible. In order to obtain higher diffraction times, it is necessary to build a reading head to carry the diffraction light path. The internal light path structure of the reading head selected in this paper is shown in Figure 2.

The incident angle and diffraction angle meet the following requirements:

$$g(\sin\theta_i + \sin\theta_k) = k\lambda, k = 0, \pm1, \pm2 \quad (1)$$

Diffraction above the second order achieves significant attenuation and is not conducive to an optical signal acquisition; therefore, this paper uses positive and negative first-order diffracted light as the measured beam. The output frequencies of the laser beams are f_1 and f_2, the frequency difference between f_1 and f_2 is a fixed value, also known as the laser differential frequency and the linear polarization

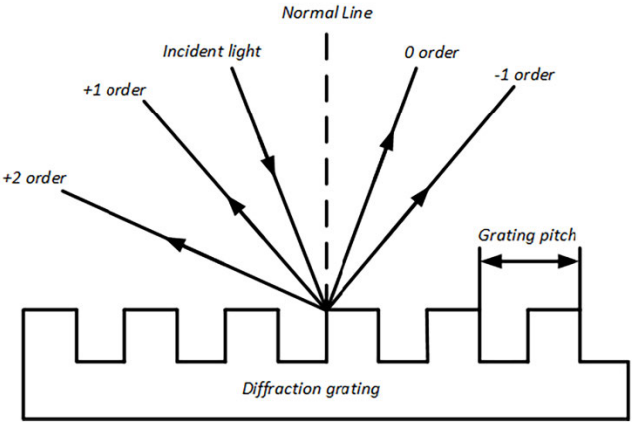

FIGURE 1. Diffraction characteristics of the grating.

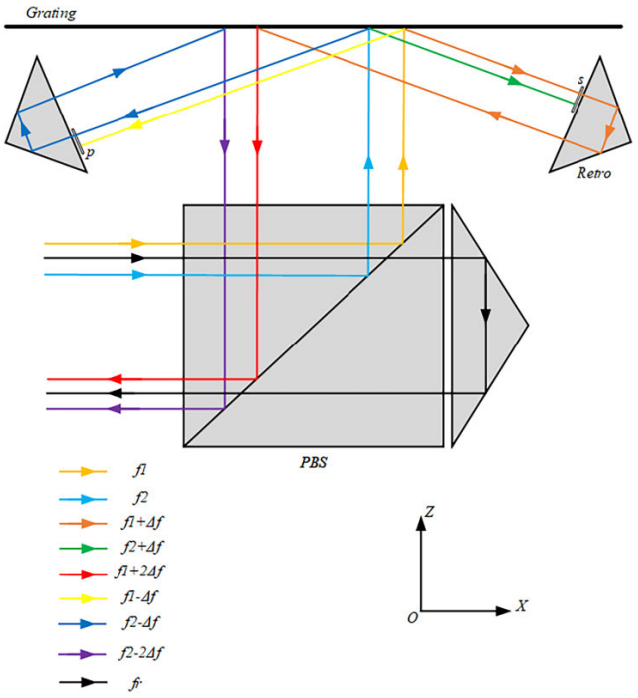

FIGURE 2. Light path inside the reading head.

directions are perpendicular to each other. When the measured beam enters the grating head, there are two diffractions on the surface of the plane grating [18].

Inside the reading head, P and S polarizers are arranged in front of two symmetrical corner prisms. When the dual-frequency laser is vertically incident on the plane grating and diffracts, only the linearly polarized light of P and S enters the corner prism after the diffracted light passes through the P and S polarizers.

Taking the XOZ plane as an example, when the plane grating moves at velocity V, the frequency of the incident light changes as follows:

$$f_{ix} = f_0(1 + \frac{v_x \sin\theta_i}{c}) \quad (2)$$

$$f_{iz} = f_0(1 + \frac{v_z \sin\theta_i}{c}) \tag{3}$$

The frequency change of the positive and negative first-order diffraction light is as follows:

$$f_{1x} = f_0(1 + \frac{v_x \sin\theta_i}{c})(1 + \frac{v_x \sin\theta_1}{c}) \tag{4}$$

$$f_{1z} = f_0(1 + \frac{v_z \cos\theta_i}{c})(1 + \frac{v_z \sin\theta_1}{c}) \tag{5}$$

The moving speed of the plane grating is limited by the 6-DOF motion table, and the maximum speed cannot exceed 1.2 m/s, which is significantly less than the speed of light, and thus the high-order term can be omitted.

$$f_{1x} = f_0(1 + \frac{v_x \sin\theta_i}{c} + \frac{v_x \sin\theta_1}{c}) \tag{6}$$

$$f_{1z} = f_0(1 + \frac{v_z \cos\theta_i}{c} + \frac{v_z \sin\theta_1}{c}) \tag{7}$$

The first diffraction is the difference in the light frequency which is expressed as follows:

$$\Delta f_{1x} = f_{1x} - f_0 = \frac{v_x}{\lambda}(\sin\theta_i + \sin\theta_1) \tag{8}$$

$$\Delta f_{1z} = f_{1z} - f_0 = \frac{v_z}{\lambda}(\cos\theta_i + \cos\theta_1) \tag{9}$$

Substituting the above formula into the multistage diffraction equation, the frequency difference of the second diffraction light is obtained as follows:

$$\Delta f_{2x} = 2\Delta f_{1x} = \frac{2kv_x}{p} \tag{10}$$

$$\Delta f_{1z} = 2\Delta f_{1z} = \frac{2v_z}{\lambda}(\cos\theta_i + \cos\theta_1) \tag{11}$$

The phase can be obtained by integrating the diagonal frequency, and the displacement can be obtained by integrating the velocity, and thus the corresponding relationship between the phase and displacement in the X and Z directions is as follows:

$$\Delta\varphi_{xoz} = \frac{4\pi m\Delta x}{p} + \frac{4\pi(\cos\theta_i + \cos\theta_k)\Delta z}{\lambda} \tag{12}$$

Similarly, in the Y and Z directions, we have the following:

$$\Delta\varphi_{yoz} = \frac{4\pi m\Delta y}{p} + \frac{4\pi(\cos\theta_i + \cos\theta_k)\Delta z}{\lambda} \tag{13}$$

The two optical interference signals in the reader head are transmitted to the photoelectric receiver through the optical fiber, and the photoelectric receiver obtains the phase value of the interference signal by obtaining the light intensity signal. The two optical interference signals have coaxial waves with the same vibration direction and frequency difference of $4f$. When these signals are superimposed, they can be combined into beat frequency signals [19], as shown in Figure 3.

The light intensity of the two interference signals is expressed as follows:

$$\mathrm{E}_1 = E_0\{1 + \cos[2\pi(f_1 + 2\Delta f)t]\} \tag{14}$$

$$\mathrm{E}_2 = E_0\{1 + \cos[2\pi(f_2 - 2\Delta f)t]\} \tag{15}$$

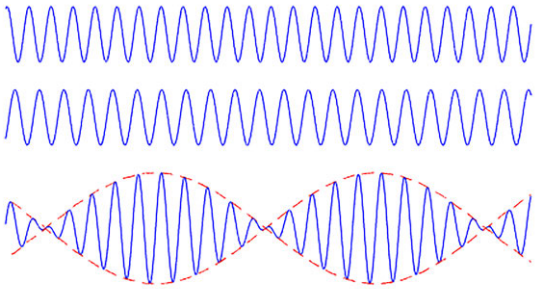

FIGURE 3. Schematic of beat frequency phenomenon.

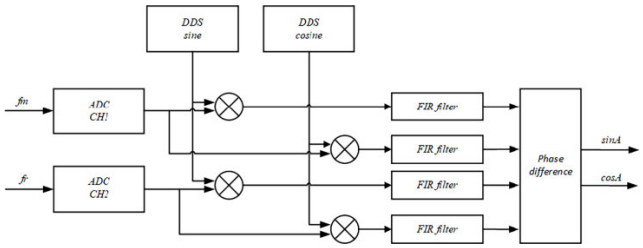

FIGURE 4. Overall structural diagram of preprocess.

The relationship between a beat frequency signal and an interference signal is as follows:

$$I = EE^* \tag{16}$$

$$I = 2E_0^2\{1 + \cos[2\pi(f_1 - f_2 + 4\Delta f)t]\} \tag{17}$$

III. PREPROCESS

The output measurement signal of a grating is a sine signal, and the frequency is the sum of the laser differential frequency and Doppler frequency shift. Under ideal conditions, the laser differential frequency should be 20 MHz. However, in practice, the ZMI 7702 laser head has a frequency uncertainty of ±1600 Hz. Because of the non-ideality of the laser intensity, laser beam overlap ratio, and elliptic polarization, among other factors, the amplitude of the sine signal is uncertain. The fact that both the frequency and amplitude are uncertain results in serious errors when calculating the phase, and a preprocess is therefore needed [20]. The overall structural diagram of preprocess base on biorthogonal lock-in amplifier is shown in Figure 4.

Suppose that the frequency of the reference signal is f_r, frequency of the measurement signal is f_m, two-frequency laser beams are f_1 and f_2, frequency uncertainty of the laser head is f', frequency difference caused by the Doppler frequency shift is Δf, amplitude coefficient of the reference signal is R, and amplitude coefficient of the measurement signal is M.

Then the reference and measurement signals can be expressed as follows:

$$f_r = R \cdot \sin[(f_1 - f_2 + f')t] \tag{18}$$

$$f_m = M \cdot \sin[(f_1 - f_2 + f' + \Delta f)t] \tag{19}$$

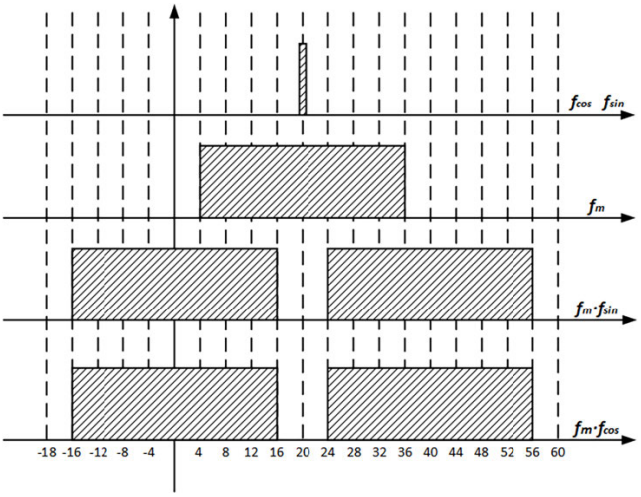

FIGURE 5. Frequency spectrum distribution of signal.

The sine and cosine signals of 20 MHz generated by the DDS are as follows:

$$f_{\sin} = \sin[(f_1 - f_2)t] \tag{20}$$

$$f_{\cos} = \cos[(f_1 - f_2)t] \tag{21}$$

The frequency spectrum distribution of the signal before and after mixing is shown in Figure 5.

Four mixing signals after low-pass filtered are as follows:

$$f_r \cdot f_{\sin} = \frac{1}{2}R \cdot \cos(f't) \tag{22}$$

$$f_r \cdot f_{\cos} = \frac{1}{2}R \cdot \sin(f't) \tag{23}$$

$$f_m \cdot f_{\sin} = \frac{1}{2}M \cdot \cos[(f' + \Delta f)t] \tag{24}$$

$$f_m \cdot f_{\cos} = \frac{1}{2}M \cdot \sin[(f' + \Delta f)t] \tag{25}$$

Using the trigonometric function difference formula, the influence of the frequency uncertainty of the laser head can be eliminated as follows:

$$(f_m \cdot f_{\cos}) \cdot (f_r \cdot f_{\sin}) - (f_m \cdot f_{\sin}) \cdot (f_r \cdot f_{\cos}) = \frac{1}{4}RM \cdot \sin(\Delta f t) \tag{26}$$

$$(f_m \cdot f_{\sin}) \cdot (f_r \cdot f_{\sin}) - (f_m \cdot f_{\cos}) \cdot (f_r \cdot f_{\cos}) = \frac{1}{4}RM \cdot \cos(\Delta f t) \tag{27}$$

We then obtain a pair of sine and cosine signals that only carry the information of the Doppler frequency shift. If the laser head is replaced, only the DDS frequency in the preprocessing module needs to be dynamically adjusted.

The use of the CORDIC algorithm to calculate the inverse trigonometric function is essentially the operation of the tangent value, and the amplitude coefficients of these two signals are the same, which implies that R and M will be suppressed during the CORDIC operation.

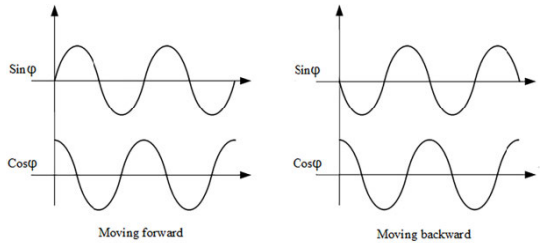

FIGURE 6. Doppler carrier for different directions of movement.

TABLE 1. The quadrant judgment results when the object is moving forward.

Sign of sine	Sign of cosine	Quadrant
Positive	Positive	1
Positive	Negative	2
Negative	Positive	3
Negative	Negative	4

TABLE 2. The quadrant judgment results when the object is moving backward.

Sign of sine	Sign of cosine	Quadrant	True quadrant
Positive	Positive	4	1
Positive	Negative	3	2
Negative	Positive	2	3
Negative	Negative	1	4

IV. DESIGN OF DIRECTION JUDGMENT SYSTEM

A. COMPENSATION PRINCIPLE OF DIRECTION JUDGMENT APPLIED TO THE PHASE

In general, we use the coordinate rotation digital computer (CORDIC) algorithm to calculate the trigonometric function [21]. The basic idea of CORDIC is to use a series of angles related only to the cardinality of an operation to approach the target angle using a constant deflection. The calculation only requires an addition and shift to be applied, and thus it can satisfy the requirement of the hardware platform.

The Doppler carrier for different directions of movement is shown in Figure 6.

When the object is moving backward, the Doppler shift is negative. According to the properties of the trigonometric function:

$$\sin[(-\Delta f)t] = -\sin[(\Delta f)t] \tag{28}$$

$$\cos[(-\Delta f)t] = \cos[(\Delta f)t] \tag{29}$$

Once the sine wave turns into a negative sine wave, the first step of CORDIC, which is known as quadrant judgment, will fail. The quadrant judgment results when the object is moving forward are listed in Table 1.

The quadrant judgment results during the backward movement of object are listed in Table 2.

It is difficult to determine whether the sine wave is negative without a direction judgment. Moreover, the convergence range of CORDIC is $[-99.88°, 99.88°]$, which implies that to calculate a complete cycle of $[-\pi, \pi]$, we need to judge the quadrant of the trigonometric function first [22], and then

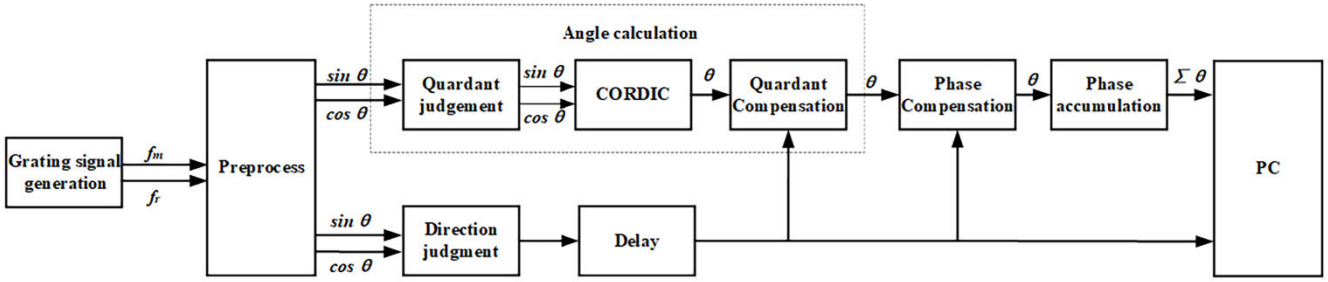

FIGURE 7. The direction judgment compensation method for the phase.

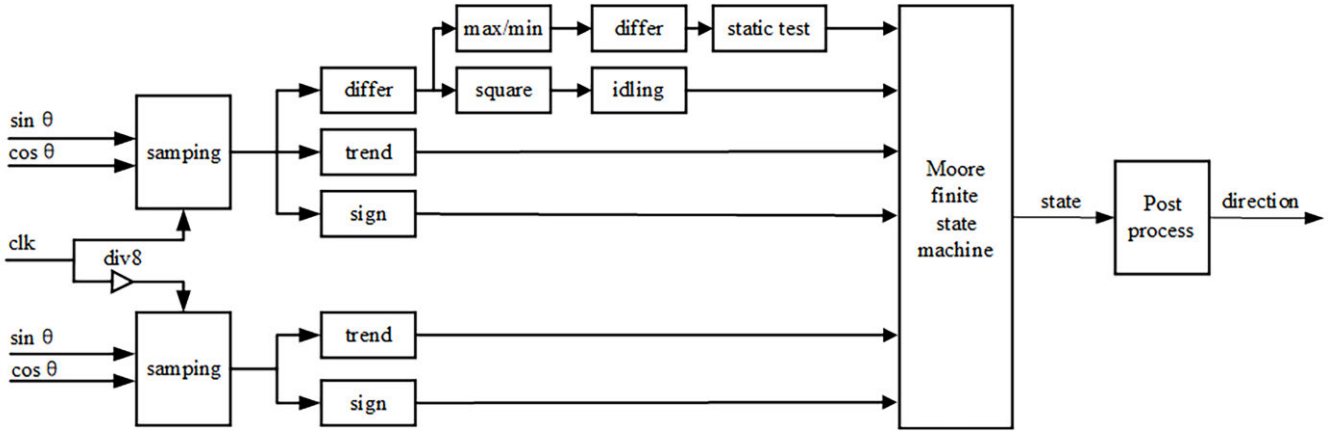

FIGURE 8. Overall structural diagram of direction judgment system.

shift the trigonometric function to the first quadrant. Without the direction judgment result, CORDIC algorithm cannot be compensated according to the quadrant information after the calculation is completed.

In addition, for the corresponding relationship between the phase and displacement, the forward moving phase should be accumulated to obtain the displacement, whereas the backward moving phase needs to be inverse accumulated. If the direction identification information cannot be updated in time, the final displacement information will be incorrect.

According to the above principle, the direction judgment compensation method for the phase is designed, a flow chart of which is shown in Figure 7.

As can be seen from Figure 7, after preprocessing the grating ruler measurement and reference signals, two groups of sine and cosine signals, including the Doppler frequency shift, are obtained. After using the CORDIC algorithm to calculate the phase, the motion direction of each point is synchronously delayed according to the CORDIC pipeline series, and the quadrant compensation signal is obtained. The phase signal after compensation determines the positive and negative phase accumulation according to the direction.

B. DESIGN OF DIRECTION JUDGMENT SYSTEM

The overall process of the direction identification system is shown in Figure 8.

Four D flip-flops are used to delay two cycles for two input signals, and supposing that the input signal is A, the output of the first-stage D flip-flop is B, and the output of the second stage D flip-flop is C. To obtain the changing trend of the input signals, A and B, B and C are compared using comparators.

TABLE 3. The four basic changing trends.

Compare result	Representation	Changing trend
a>b & b>c	11	Increase
a>b & b>c	00	Decrease
a>b & b>c	01	Keep
a>b & b>c	10	Keep

When the Doppler frequency shift is less than 100 kHz, limited by the ADC sampling rate, it cannot be guaranteed that each clock cycle has a change in signal amplitude. At this time, an 8-division clock is used to sample the input signal and detect the amplitude changing trend between every 8 clock cycles, which can allow the system to maintain the direction judgment ability when the Doppler frequency shift is extremely low.

The four basic changing trends are listed in Table 3. According to the positive and negative signs of the sign bit and the changing trend of the input signals, a direction judgment can be realized in real-time. The correspondence of the sign bit, changing trend, and direction are shown in Table 4.

The object motion direction switching needs to pass through a zero velocity; the Doppler frequency shift at zero velocity is 0, and the signal is a direct current. At this time,

TABLE 4. The correspondence of the sign bit, changing trend, and direction.

Sign of sine	Sign of cosine	Trend of sine	Trend of cosine	Direction
Positive	Positive	Increase	Decrease	Forward
Positive	Negative	Decrease	Decrease	Forward
Negative	Negative	Decrease	Increase	Forward
Negative	Positive	Increase	Increase	Forward
Negative	Positive	Decrease	Decrease	Backward
Negative	Negative	Increase	Decrease	Backward
Positive	Negative	Increase	Increase	Backward
Positive	Positive	Decrease	Increase	Backward

A should equal to B, but it is unreasonable to directly take B-A = 0 as the criterion of a Doppler frequency shift to 0.

The input sine and cosine differ to obtain Δ sin and Δ cos as follows:

$$\Delta \sin(\varphi) = \sin[\omega(t + \Delta t)] - \sin(\omega t) \tag{30}$$

$$\Delta \cos(\varphi) = \cos[\omega(t + \Delta t)] - \cos(\omega t) \tag{31}$$

where Δt is the unit sampling time interval, and the difference product can be obtained through the following equations:

$$\Delta \sin(\varphi) = 2\cos[\omega(t + \frac{\Delta t}{2})] \cdot \sin(\frac{\omega \Delta t}{2}) \tag{32}$$

$$\Delta \cos(\varphi) = -2\sin[\omega(t + \frac{\Delta t}{2})] \cdot \sin(\frac{\omega \Delta t}{2}) \tag{33}$$

It can be seen from formula (32) and (33) that the difference signal is essentially a sine and cosine pair, and that the sine and cosine have zero crossing points; that is, when there is a Doppler frequency shift that is not zero, b−a will still incur a state equal to zero. Based on this principle, the lower the frequency difference function, the smaller is the amplitude difference function:

$$S = \Delta \sin^2(\varphi) + \Delta \cos^2(\varphi) \tag{34}$$

Because of the noise in the input signal, S cannot be completely zero. When S is less than or equal to the preset threshold, the amplitude of the differential signal is less than the amount of noise, which implies that the object is in a state of static or extremely low-speed motion. At this time, the state is called the idle state. In an idle state, the phase is still updated according to the original state.

The noise amplitude is controlled within ± 1 LSB by an appropriate truncation, and the maximum and minimum values of the input signal are then detected in an idling state. If the absolute value of the difference between the maximum and minimum values of the input signal is less than or equal to 1 in 128 clock cycles, it can be considered that the plane grating is in a completely static state.

In this paper, a zero indicates that the sign bit is positive, 1 indicates that the sign bit is negative, and the expression method for an increased, decreased, and maintained value is consistent with that shown in Table 3.

The state variable has a total of 8 bits, and is composed of symbol signal, changing trend, static flag and idling flag, and x indicates that the state variable is unimportant. When the state machine is not in an idling state, the idling flag signal has the highest priority. When the state machine is in an idling state, the static flag signal has the highest priority. The flow chart of the state machine is shown in Figure 9. Every 6 bits of 4 rows are arranged in the following order: sine symbol, cosine symbol, sine changing trend and cosine changing trend.

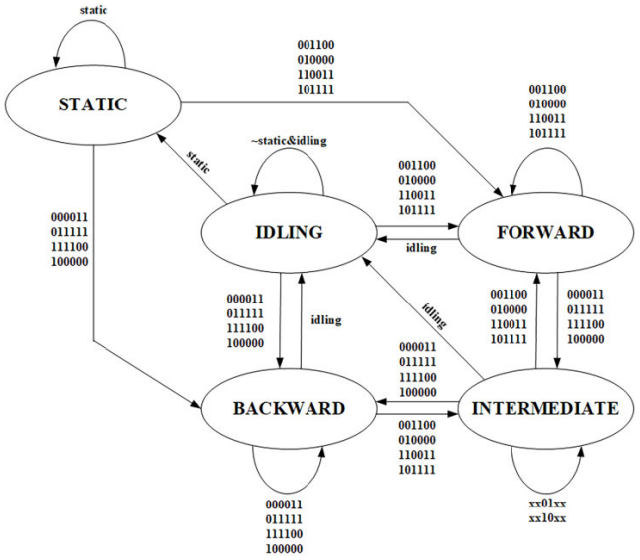

FIGURE 9. Flow chart of state machine.

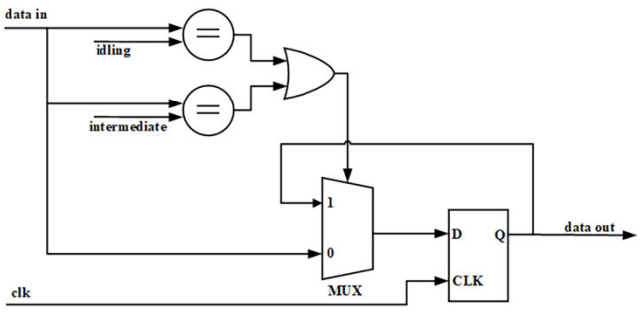

FIGURE 10. Post-processing structure of the system.

The real-time direction judgment module is realized using a Moore state machine, and the output motion direction information is only related to the current state and has no relation with the input signal. Compared with the Mealy state machine, the resource consumption is further reduced.

It should be note that jumping from a forward or backward state to an intermediate state does not imply that they are no longer in the forward or reverse state. An intermediate state aims at the peaks and troughs of the sine and cosine signals. When the plane grating moves to the peak, the oversampled signal will have a clock cycle of $A < B$ and $B > C$, which does not meet the changing trend listed in Table 2; however, the plane grating still retains the original motion state. This requires an intermediate state to eliminate the impact of this jump. The post-processing structure of the system is shown in Figure 10.

Resource	Estimation	Available	Utilization %
LUT	232	203800	0.11
FF	181	407600	0.04
DSP	2	840	0.24
IO	33	500	6.60
BUFG	1	32	3.13

FIGURE 11. Resource requirements of the direction judgment system.

Resource	Utilization	Available	Utilization %
LUT	22654	203800	11.12
LUTRAM	229	64000	0.36
FF	23552	407600	5.78
BRAM	321.50	445	72.25
DSP	222	840	26.43
IO	38	500	7.60
BUFG	5	32	15.63
MMCM	1	10	10.00

FIGURE 12. Resource requirements of the complete electronic subdivision system.

Because the motion direction switching must first pass a zero velocity, when such a velocity is not detected, that is, if the state is intermediate or idle, the output of the previous state will be maintained. When the direction judgment state machine jumps directly from forward or backward to idling state or intermediate state under the influence of noise, it can be inferred that the grating motion direction has not been switched because it has not passed the static state. Under the function of post-processing module, the output value of error jump is kept as the original output, which makes the direction judgment system robust.

C. COMPILATION RESULTS

The resource requirements of the direction judgment system according to the compilation results are listed in Figure 11. The resource requirements of the entire electronic subdivision system include preprocessing, direction judgment, phase calculation, phase compensation, Gigabit Ethernet lower computer transmission, and other functions, are listed in Figure 12. The Gigabit Ethernet transmission has a significant impact on FPGA resource utilization.

The Gigabit Ethernet transmission has a significant impact on FPGA resource utilization. Figure 13. shows the comparison of the proportion of logical resources occupied by the direction judgment system and the complete electronic subdivision system without Gigabit Ethernet transmission for all resources of Xilinx Kintex-7 325t.

In FPGA, flip-flop (FF) is used to realize sequential logic, look-up table (LUT) is used to realize combinational logic, and digital signal processor (DSP) module is used to realize complex multiplication. It can be seen from Figure 13 that the LUT, DFF, and DSP occupied by the direction judgment system are less than 10% of the entire system. This implies that the system will not be overburdened.

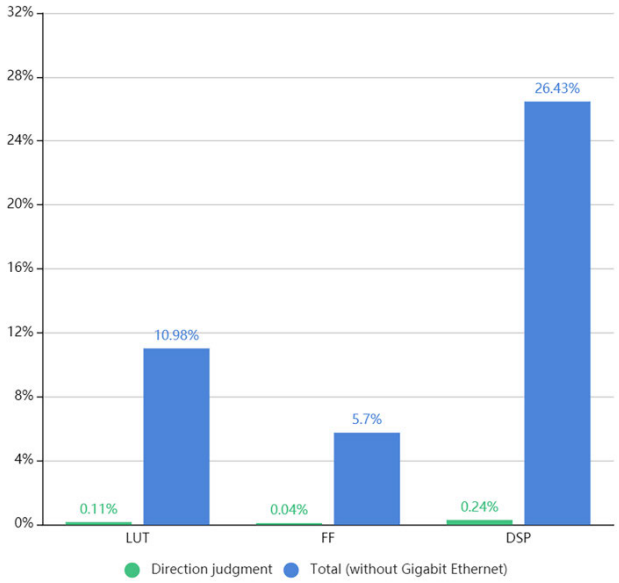

FIGURE 13. Resource comparison.

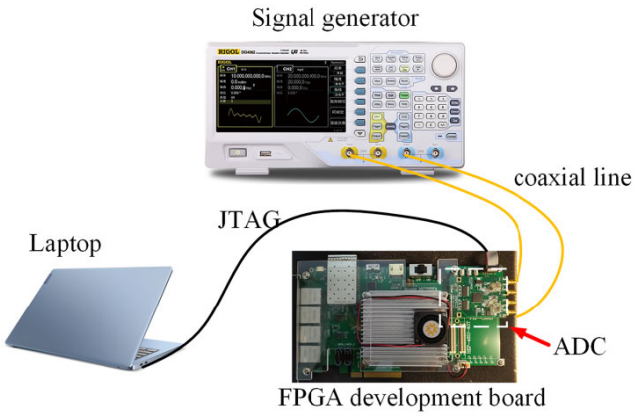

FIGURE 14. Experimental platform.

V. EXPERIMENTAL RESULTS

The real-time direction judgment system is a subsystem of the electronic subdivision system. In this paper, the function of the real-time direction judgment system is tested by replacing the photoelectric signal of the plane grating with the signal generated by the signal generator.

The experimental platform uses a DG4062 signal generator and MK7325FA FPGA development board, as shown in the Figure 14. The FPGA chip model of the development board is an XC7K325T-FFG900-2I and a 12-bit ADC chip with a sampling rate of 125 MSa/s is used to obtain the input signal. In the Vivado 2019.1 development environment, Verilog HDL language is used to design the direction judgment algorithm circuit, which is downloaded into the FPGA chip to complete the direction judgment function.

A. COMPENSATION PRINCIPLE OF DIRECTION JUDGMENT APPLIED TO THE PHASE

When the plane grating moves in the forward direction, the Doppler frequency shift is positive, and the maximum

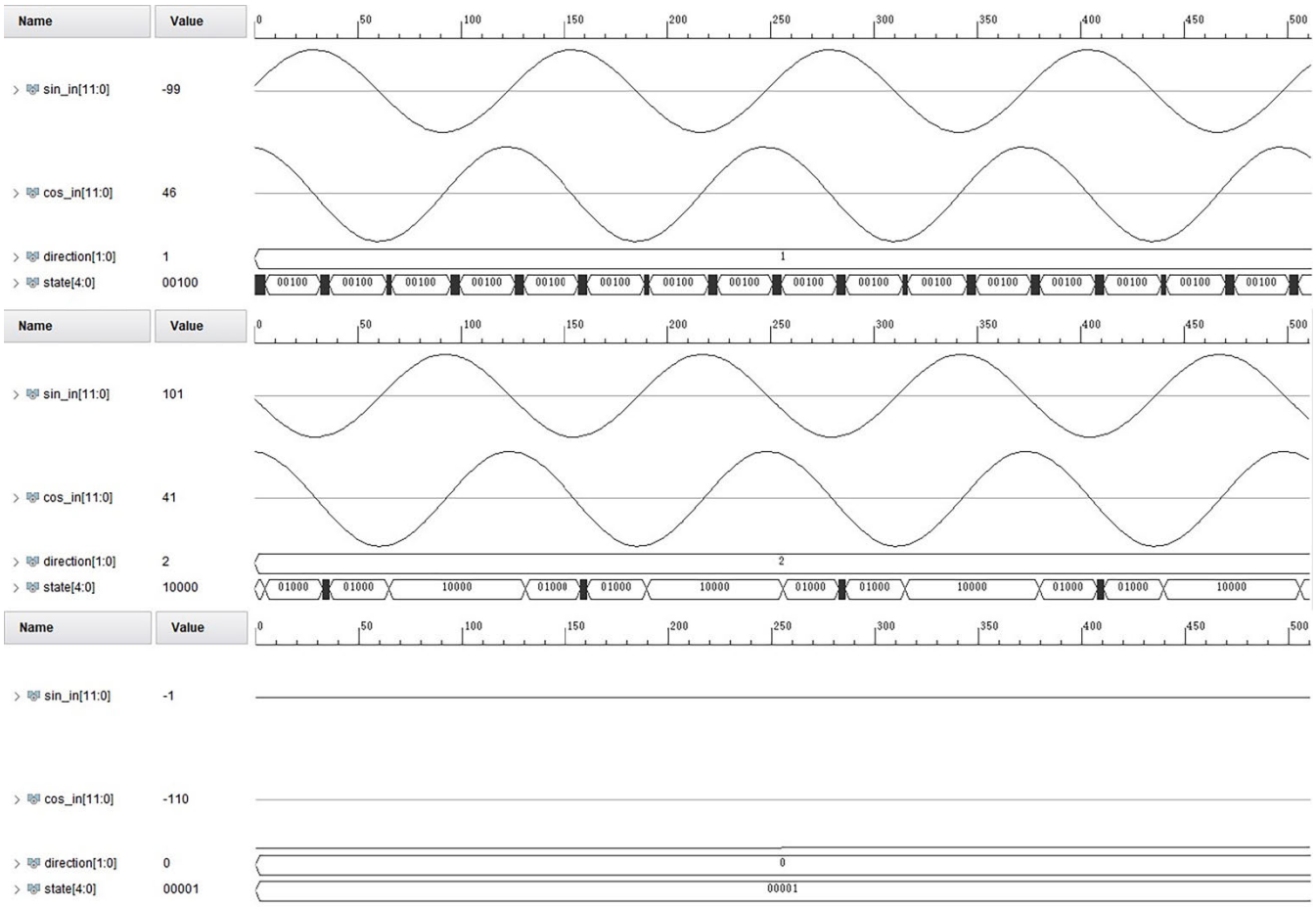

FIGURE 15. Experiment results of stationary motion.

moving speed is 1.2 m/s, corresponding to a frequency shift of 16 MHz. Therefore, the measured signal is a sine wave of greater than 4 MHz and less than or equal to 36 MHz, and the reference signal is a sine wave of 20 MHz.

The input measurement signal from 4 to 36 MHz is verified. Among them, the specified direction of zero is static, 1 is positive, and 2 is negative. The state of the state machine is encoded by one-hot code, ''00001'' stands for static state, ''00010'' stands for idling state, ''00100'' stands for forward state, ''01000'' stands for backward state, and ''10000'' stands for intermediate state.

Figure 15. shows the direction judgment results when the measured signals are 19, 21, and 20 MHz, respectively. The acquisition mode uses an integrated logic analyzer (ILA), and the number of sampling points is 131,072.

B. VALIDATION OF EFFECTIVENESS OF MOTION DIRECTION SWITCHING

When the plane grating is in static condition, the Doppler frequency shift is zero, and the input signal is the difference frequency of 20 MHz of the dual-frequency laser. After preprocessing, the DC output is obtained.

For the real-time direction judgment system, each input measurement signal has a corresponding direction judgment result. Theoretically, there is no limit to switching frequency. Limited by the performance of the motion platform, the maximum acceleration of the plane grating is 32 m/s^2. In the forward-to-reverse direction switching experiment, the test case is implemented using a 21 to 19 MHz frequency sweep. The signal frequency of 21 MHz is the superposition of laser frequency difference of 20 MHz and Doppler frequency shift of 1 MHz. The Doppler frequency shift of 1 MHz can be calculated according to formula (10), the velocity of plane grating is 0.75 m/s. Similarly, the corresponding velocity of 19 MHz is -0.75 m/s. When the plane grating moves from 0.75 m/s to -0.75 m/s with 32 m/s^2 acceleration, the total time consumed is 4.6875 ms, so the sweep time is set to 4.6875 ms. The experimental results are shown in Figure 16.

The forward motion decelerates to rest, and then continues to move forward. The test case is implemented using a 21 MHz $\rightarrow$ 20 MHz $\rightarrow$ 21 MHz frequency sweep.

Reverse movement decelerates to rest, and then continues the reverse movement. The test case is implemented using a 19 MHz $\rightarrow$ 20 MHz $\rightarrow$ 19 MHz frequency sweep.

In the above experiments, the signal generator is used to generate test cases for various possible motion states of the plane grating, and the correct direction judgment results

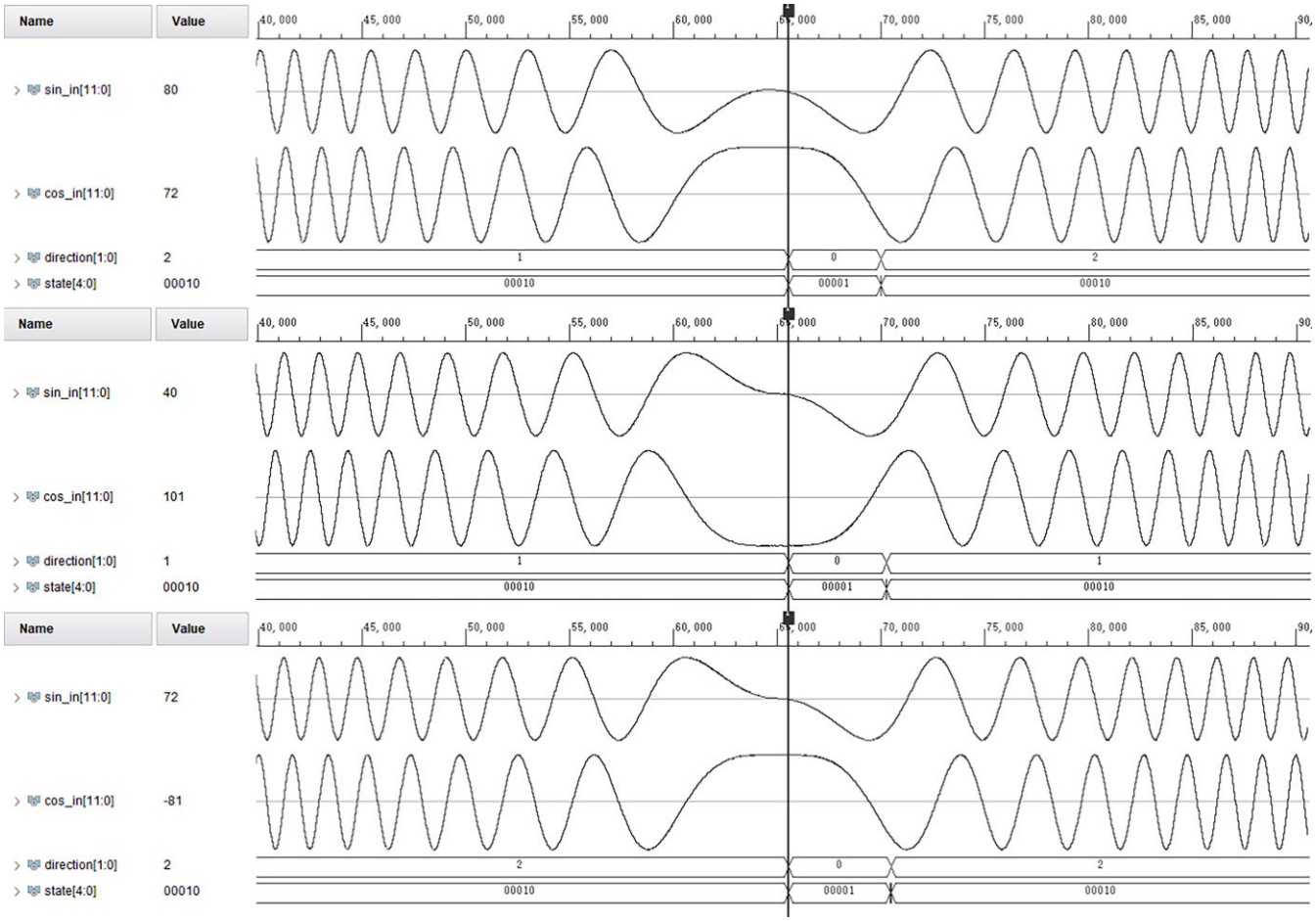

FIGURE 16. Experimental results of motion direction switch.

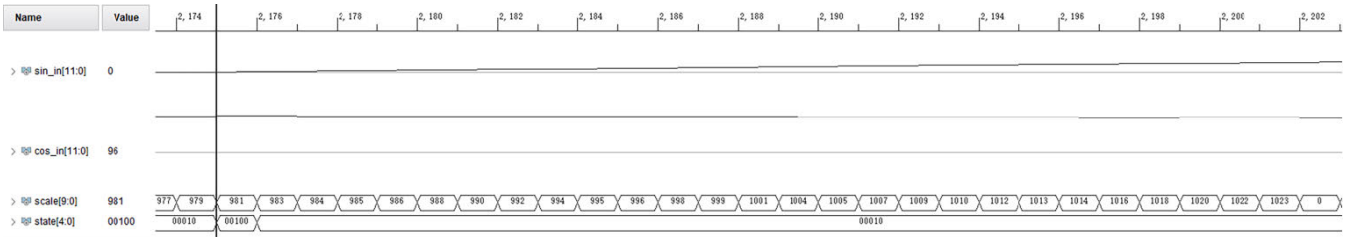

FIGURE 17. Experimental results of the data update rate of direction judgment system.

can be obtained. The experimental results demonstrate the effectiveness of the system.

In order to test the response speed of the direction judgment system, an experiment of testing the data update rate of direction judgment system is proposed, the experimental result is shown in Figure 17. The working frequency of the direction judgment system is 125 MHz, and the latency is 4 clock cycles, same as 32 ns. Scale is the mapping value of phase from [0°, 360°] to [0, 1024] in order to facilitate the accumulation and transmission. When the electronic subdivision system is working at a data update rate of 1024 times per sinusoidal cycle, the direction judgment system can track and respond to this change in real-time. Compared with the traditional direction judgment system with the highest update rate of 4 times per sinusoidal cycle, the date update of the real-time direction judgment system is improved by 256-fold.

VI. CONCLUSION

In this study, a real-time direction judgment method of a grating ruler phase signal is proposed, and a real-time direction judgment system based on an FPGA circuit was constructed. First, the phase compensation scheme based on the result of the direction judgment is determined. Second, a signal pre-processing scheme was established. Using a mixing, filtering, and phase difference, the sine and cosine signals containing only Doppler shift information were obtained. Subsequently, a real-time direction judgment system was designed. By combining the symbol signal,

changing trend, static flag and idling flag, a Moore state machine was designed to jump the direction judgment state. A post-processing module was then designed to ensure the strong robustness of the system.

During the experimental process, the correctness of the direction judgment in uniform forward, uniform reverse, and static states was proved first, and then the effectiveness of switching from forward motion to reverse motion, from reverse motion to forward motion, from forward motion to forward motion, and from reverse motion to reverse motion was proved. The experimental results show that the direction judgment system can track the moving direction of a grating correctly and significantly improve the real-time performance of the direction judgment.

REFERENCES

[1] D. Marek, "High resolution laser transducer of liner displacement," *Opt. Eng.*, vol. 31, no. 3, pp. 500–504, 1992.
[2] L. L. Dong, J. W. Xiong, and Q. H. Wan, "Development of photoelectric rotary encoders," *Opt. Precis. Eng.*, vol. 8, no. 2, 2008, Art. no. 198202.
[3] T. T. Wu, "Development and experimental study of a multi-degree-of-freedom simultaneous measurement system for two-dimensional stage," Hefei Univ. Technol., Anhui, China, Tech. Rep., 2018, pp. 20–28.
[4] C.-H. Liu, W.-Y. Jywe, C.-C. Hsu, and T.-H. Hsu, "Development of a laser-based high-precision six-degrees-of-freedom motion errors measuring system for linear stage," *Rev. Sci. Instrum.*, vol. 76, no. 5, May 2005, Art. no. 055110.
[5] Z. Zhang and C.-H. Menq, "Laser interferometric system for six-axis motion measurement," *Rev. Sci. Instrum.*, vol. 78, no. 8, Aug. 2007, Art. no. 083107.
[6] S. Mao, "Key technologies study of dynamic displacement calibration for high speed heterodyne laser interferometer based on the same measurement trajectory," Harbin Inst. Technol., Harbin, China, 2017, Tech. Rep., pp. 56–82.
[7] P. T. Konkola, "Design and analysis of a scanning beam interference lithography system for patterning gratings with nanometer-level distortions," Massachusetts Inst. Technol., Boston, MA, USA, Tech. Rep., 2003.
[8] T. Castenmiller, F. van de Mast, T. de Kort, C. van de Vin, M. de Wit, R. Stegen, and S. van Cleef, "Towards ultimate optical lithography with NXT: 1950i dual stage immersion platform," *Proc. SPIE*, vol. 7640, Mar. 2010, Art. no. 76401N.
[9] X. Li, W. Gao, H. Muto, Y. Shimizu, S. Ito, and S. Dian, "A six-degree-of-freedom surface encoder for precision positioning of a planar motion stage," *Precis. Eng.*, vol. 37, no. 3, pp. 771–781, Jul. 2013.
[10] Y. Huang, Z. Xue, M. Huang, and D. Qiao, "The NIM continuous full circle angle standard," *Meas. Sci. Technol.*, vol. 29, no. 7, Jul. 2018, Art. no. 074013.
[11] Y. Huang, Z. Xue, D. Qiao, and Y. Wang, "Study on the metrological performance of self-calibration angle encoder," *Proc. SPIE*, vol. 9684, Sep. 2016, Art. no. 968400.
[12] W. Kokuyama, T. Watanabe, H. Nozato, and A. Ota, "Measurement of angle error of gyroscopes using a rotary table enhanced by self-calibratable rotary encoder," in *Proc. IEEE Int. Symp. Inertial Sensors Syst.*, Mar. 2015, pp. 1–4.
[13] W. Ren, J. Cui, and J. Tan, "A novel enhanced roll-angle measurement system based on a transmission grating autocollimator," *IEEE Access*, vol. 7, pp. 120929–120936, 2019.
[14] L. Huaiqiong and C. Ji, "Study on raster-sensing technology," *Optoelectron. Technol.*, vol. 19, no. 4, pp. 261–264, 1999.
[15] X. Yuqin and Z. Yong, "Grating-ruler signal based on FPGA," in *Proc. Int. Conf. Netw. Digit. Soc.*, Wenzhou, China, May 2010, pp. 422–424, doi: 10.1109/ICNDS.2010.5479225.
[16] H. Zhao, "Study of subdivision and direction judgment for grating signal based on FPGA," Tech. Rep., 2010.
[17] Z. Wentao *et al.*, "Hardware in the-Loop Simulation of High Precision Displacement Measurement System," *Chin. J. Lasers*, vol. 46, no. 02, 2019, Art. no. 0204001.
[18] D. Baosheng, X. Xianming, W. Xianying, and Z. Wentao, "Ultra-precision encoder system for displacement measurement," *Laser Journal*, vol. 39, no. 9, pp. 42–46, 2018.
[19] S. Mingyang, "Study on a displacement measuring system based on phase grating interferometry," Harbin Inst. Technol., Harbin, China, Tech. Rep., 2016.
[20] C. Haijiao, "Research on picometer resolution Hase subdivision for heterody ne laser interferometer signals," Harbin Inst. Technol., Harbin, China, Tech. Rep., 2015.
[21] J. E. Volder, "The CORDIC trigonometric computing technique," *IRE Trans. Electron. Comput.*, vol. 8, no. 3, pp. 330–334, Sep. 1959.
[22] J. Mao and D. Zou, "Implementation of DDS based on CORDIC algorithm," *Radio Eng.*, vol. 12, p. 4, 2011.

SIMIN LI was born in Suzhou, China, in 1963. He received the B.E. degree in communication engineering from the Nanjing University of Posts and Telecommunications, Nanjing, China, in 1984, and the Ph.D. degree in electromagnetic field and microwave technology from the University of Electronic Science and Technology of China, Chengdu, China, in 2003. His current interests include the antenna, microwave circuit, and electromagnetic pulse communication systems.

JINGKUN WANG was born in Tangshan, China, in 1993. He received the bachelor's degree from Hangzhou Dianzi University, Hangzhou, China, in 2015. He is currently pursuing the master's degree with the Guilin University of Electronic Technology, Guilin, China. His research interest includes the grating signal processing and its applications.

WENTAO ZHANG received the Ph.D. degree from Tongji University, in 2008. He is currently a Professor with the Guilin University of Electronic Technology. His research interests include photoelectric detection technology, laser technique, and terahertz technology.

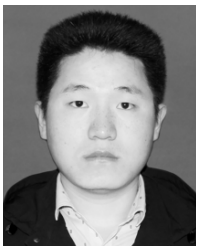

HAO DU is currently pursuing the Ph.D. degree with the Guilin University of Electronic Technology. His current research interests include grating interferometers, grating calibration, and laser interferometers.

XIANMING XIONG is currently a Research Fellow with the Guilin University of Electronic Technology. His current research interests include photoelectric test, computer aided test, and optical remote sensing test.